High Temperature Deformation and Fracture Mechanisms in a Nickel Aluminide Alloy

Kang Chung* and Ho-Kyung Kim**

(Received November 12, 1993)

The mechanisms that control high temperature deformation and fracture were studied in a nickel aluminide(Ni_3Al) alloy that was thermo-mechanically treated to produce a non-porous microstructure. Comparisons of data corresponding to the dendritic morphology with that for the equiaxed grain structures indicated that the dendritic morphology results in a significantly lower creep rates as well as substantially greater times to rupture. From the microstructural observations, isolated interdendritic cavitation in th absence of grain boundary sliding was found to lead to rupture lifetime that are longer than those observed for the other microstructures.

Key Words : Nickel Aluminide, Creep Deformation, High Temperature Facture, Dendritic Microstructure, Creep Damage Tolerance, Creep Rupture Lifetimes, Creep Cavity Damage

1. Introduction

Intermetallic compounds have recently been the subject of considerable interest for high temperature applications. In particular, Ni_3Al is one of the more promising intermetallic compounds for high temperature applications as a result of its anomalous dependence of strength on temperature, low density and good oxidation resistance (Stoloff, 1989 ; Yamamuchi et al., 1990 ; Liu et al., 1985 ; Lall et al., 1979). Also, the tensile ductility is improved with trace additions of boron in the material.

The lifetimes of engineering components which operate at elevated temperature are controlled by both creep deformation and rupture. These creep properties depend on such factors as alloying elements, operating temperature, environmental conditions and microstructures. A great deal is now known about elevated temperature tensile properties and the effect of adding different alloying elements in Ni_3Al (Stoloff, 1989 ; Liu et al., 1985 ; Lall et al., 1979 ; Izumi and Takasugi, 1988 ; Milligan et al., 1989).

However, the mechanisms controlling creep rupture in intermetallics have received little attention. Even though the baseline properties of intermetallic materials are continuously being improved, their successful applications require a better understanding of both the creep deformation and rupture processes. Furthermore, a knowledge of the relationships between microstructure and high temperature properties in these alloys are needed to enable the development of optimum microstructures for a given set of conditions.

The objective of the present study was to develop a better understanding of the nature of creep deformation and high temperature fracture mechanisms in Ni_3Al alloys with a dendritic grain structure. Emphasis is placed in the present investigation on the effects of grain morphology on high temperature deformation and fracture mechanisms in a Ni_3Al alloy.

* Department of Mechanical Engineering, Yosu National Fisheries University, 195, Kook-dong, Yosu-si, Chonnam

** Hong-ik University, Tribology Research Center 72-1, Sangsu-dong, Mapo-gu, Seoul-si

2. Experimental

2.1 Material and heat treatments

The nominal composition of the Ni_3Al alloy, designated as IC396, used in the present study is 8.0 Al, 7.7 Cr, 3.0 Mo, 0.85 Zr, 0.005 B, bal Ni(in wt. pct.). At high temperature, Ni_3Al is susceptible to a form of intergranular brittleness due to the action of oxygen known as dynamic embrittlement (Stoloff, 1989). The addition of about 8 wt% Cr to the alloy has been found to reduce this embrittlement significantly by forming a protective oxide film while yielding about 10 to 15 % of the disordered Ni-rich γ phase under equilibrium conditions (Stoloff, 1989). In this aluminide, molybdenum and zirconium are also added to improve the high temperature strength via solid-solution hardening effects. It has been suggested that addition of zirconium to Ni_3Al also reduces the grain boundary diffusivity by a factor of about 5 which would significantly reduce cavity growth rates (Stoloff, 1989). Microalloying with boron increases ductility at ambient temperatures as mentioned before. In the present investigation, four different grain morphologies were produced by thermomechanical treatments ; (1) dendritic, (2) fine equiaxed grain, (3) equiaxed grains containing a rosette shape of γ phase and (4) equiaxed grains containing a network of γ phase. The treatments used to produce each microstructure are summarized in Table 1.

The microstructure of IC396 in the as-cast condition, shown in Fig. 1, consists of primary dendrite arms which grew radially from the surface to the center of the cast cylinders. We note that the resulting dendrite arms are locked in the microstructure in manner similar to the pieces of a "jig-saw" puzzle. A hot isostatic pressing(HIP) treatment was performed to shrink casting pores. Metallographic evidence indicates that the larger pores are reduced in size while those that are small are removed by sintering during this treatment. The dendritic grains consist of either Ni_3Al(γ' phase) or the Ni-rich γ phase interspersed with γ' in a lamelar structure. In general, as-cast polycrystalline solids have several distinct zones with different grain microstructures due to the gradient in cooling rates during solidification. To avoid this variation in microstructure, specimens were machined from locations that were approximately the same radial distance from the center of the casting used in the present work. The tensile properties of the dendritic material are given in Table 2 indicating that, although dendritic microstructures sometimes give rise to a brittle behavior, a room temperature tensile ductility of 17% was achieved with the present microstructure. The present alloy was also hot extruded to yield a 0.33 inch diameter rod with a fine grain size resulting from recrystallization. A typical micrograph of this fine grain structure is shown in Fig. 2. The hot extruded alloy was annealed for different periods and temperatures and water quenched to increase the grain size. Annealing at 1273 K for 100 h followed by water quenching produced an $\gamma-\gamma'$ microstructure, referred to here as a rosette microstructure, as shown in Fig. 3. This microstructure consists of disordered γ islands within an ordered γ' matrix. The protruding white regions in Fig. 3 consist of the disordered γ phase and the dark regions consist of the ordered γ' phase. The result of an energy dispersive spectroscopy(EDS) analysis showed that the disordered γ phase contains a higher Cr concentration, compared to the γ' phase. The volume fraction of γ phase,

Table 1 Thermomechanical treatments used in the present investigation

Microstructure	Treatment	Grain size
Dendritic	Hipped (1408 K, 104 MPa, 4 h)	
Fine grained	As-Extruded (9 : 1)	2 μm
Rosette	Extrusion + Annealing (1277 K, 100 h) + Water Quenching	20 μm
Network	Extrusion + Annealing (1373 K, 50 h) + Water Quenching	20 μm

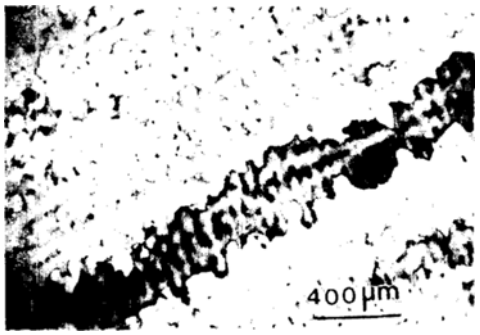

Fig. 1 Micrograph showing the Ni_3Al (Cr, Mo, Zr, B) alloy with the dendritic microstructure

Table 2 Room temperature tensile properties of the present dendritic microstructure

Yield strength	Ultimate strength	Strain to failure
360 MPa	707 MPa	0.17

Fig. 2 Micrograph showing the Ni_3Al (Cr, Mo, Zr, B) alloy the fine grained microstructure

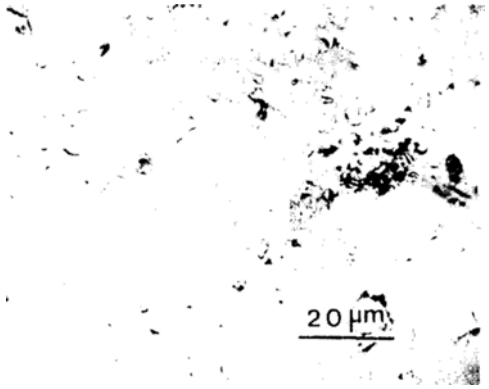

Fig. 3 Micrograph showing the Ni_3Al (Cr, Mo, Zr, B) alloy with the g rosette microstructure

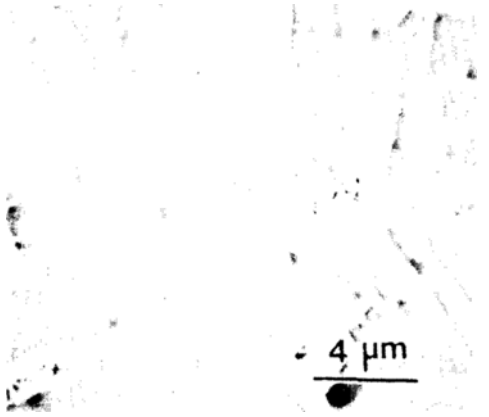

Fig. 4 Micrograph showing the Ni_3Al (Cr, Mo, Zr, B) alloy with the g network microstructure

higher than the expected (e.g. 10~15%), may be due to the non-equilibrium state by water quenching. Annealing at 1373 K for 50 h followed by water quenching produced another type of $\gamma-\gamma'$ configuration, referred to here as a network microstructure, as shown in Fig. 4. The grain size for both the rosette and network microstructures in approximately 20 μm.

2.2 High temperature testing

Tensile type creep specimens were ground to size with a gage diameter and length of 3.18 mm and 15.88 mm, respectively. The specimens were tested under constant tensile stress conditions ranging from 300 to 800 MPa at 1033 K in a vacuum environment of 10^{-3} Pa, using a custom-built high temperature testing system. Fracture surfaces and longitudinal sections of the specimens were examined using scanning electron microscope(SEM) and optical microscope to determine the extent and location of creep damage within the microstructure of the specimens.

3. Experimental Results

3.1 Creep deformation

Typical creep curves for four different microstructures tested at 1033 K are illustrated in Figs. 5 and 6. The creep curves are not similar to those typically observed for other Ni_3Al alloys in that the materials exhibited constant strain rate behavior with little indication of accelerating or inverse creep (Schneibel et al., 1989). The curve shapes

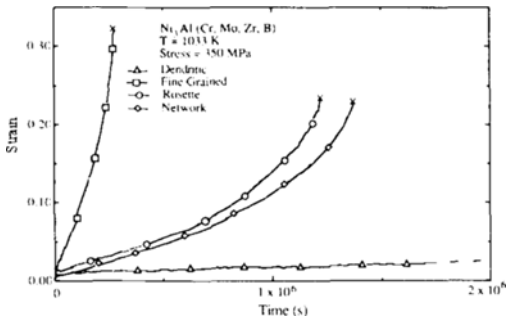

Fig. 5 Typical creep strain versus time curves for the IC 396 alloy with different microstructure under 350 MPA

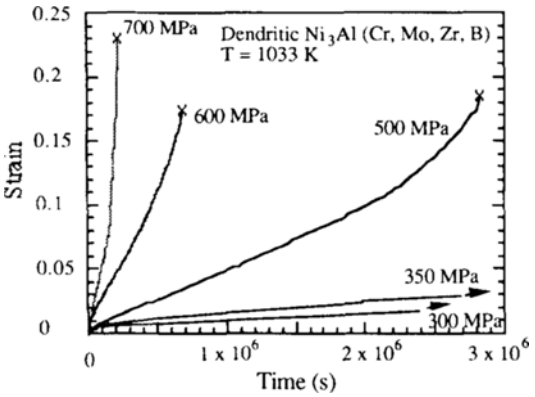

Fig. 6 Typical creep strain versus time curves for dendritic Ni_3Al (Cr, Mo, Zr, B)

are also not similar to those for superalloys which exhibit long tertiary creep due to microstructural softening (MacKay et al., 1985).

The effect of mircrostructure on steady state creep rate as a function of applied strees is shown in Fig. 7. The creep resistance of the dendritic microstructure is greater than that for the other microstructures. The strongest microstructure showed an advantage of at least two orders in creep resistance (i.e. steady state creep strain rates) relative to the weakest (fine grained microstructure) at 350 MPa by extrapolating the lines even different stress exponents. Compared with fine grained cast material, the rosette and network microstructures were stronger under creep conditions, apparently due to their larger grain size. Network microstructure was not significantly stronger than the rosette microstructure. This

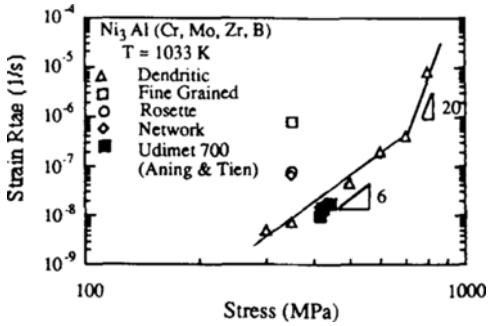

Fig. 7 Strain rate versus applied stress for Ni_3Al (Cr, Mo, Zr, B) specimens

indicates that the morphology and configuration of the γ phase had little effect on the creep properties of these microstructures. A least square fit of the data in this figure for the dendritic specimens under intermediate stresses gives power law creep constants of

$$\dot{\epsilon} = 5.9 \times 10^{-24} \sigma^{6.0} \qquad (1)$$

where $\dot{\epsilon}$ and σ are in units of s^{-1} and MPa, respectively. It can be seen in Fig. 7 that in the case of the dendritic material, the value of the stress exponent changes from 6 to about 20 at approximately 700 MPa. This suggests that above this stress either power law breakdown occurs or another creep deformation mechanism, which gives rise to a large value of n, dominates the behavior.

Creep data for a nickel-base wrought superalloy, Udimet 700 (Aning et al., 1980), tested under conditions identical to those employeed in the present investigation are plotted in Fig. 7 for comparison. The microstructure of Udimet 700 is composed of equaxed grains, having an average size of about 300 μm, containing approximately 36 vol.% cuboidal Ni_3Al precipitates (Aning et al., 1980). We note that the minimum creep rates for this relatively large grained superalloy and the present dendritic grain structure are essentially the same for a given stress.

3.2 High temperature fracture

Creep rupture lifetimes for Ni_3Al (Cr, Mo, Zr, B) specimens with different microstructures are plotted as a function of applied stress in Fig. 8. It can be seen by extrapolation of the data in this

figure that the various microstructures result in a variation of almost two magnitude in rupture lifetime. The rupture lifetime for the cast dendrite microstructure is greater than those for the equiaxed grain structures. The dendritic microstructure also exhibits rupture times that are about an order of magnitude greater than that for Udimet 700.

The ductility of the alloys at rupture showed the expected pattern of behavior Although elongations at rupture were in the range of 17～35% for the alloys, for a given composition with different microstructures, the fine grained material was the most ductile, as shown in Fig. 9. Because, the decrease in grain size will reduce stress concentrations at triple points leading to cavity nucleation and early failure during creep. In general, conventional cast alloys are expected to have poor ductility at high temperatures. It is interesting to note the good ductility in the case of dendritic material, compared to the equiaxed grain microstructures.

3.3 Creep damage and fracture metallographic observations

The creep lifetime of high temperature materials in governed by the nucleation, growth and coalescence of grain boundaries cavities which in turn leads to intergranular fracture. Thus, an understanding of these mechanisms is required to predict the lifetime of a given material and to improve its creep resistance. Longitudinal sections of the interrupted and ruptured specimens have been examined using SEM and optical micrographs to determined the extent and location of creep damage within the microstructure of the specimens.

Etched and unetched optical micrographs are shown in Figs. 10(a) and (b), for a dendritic

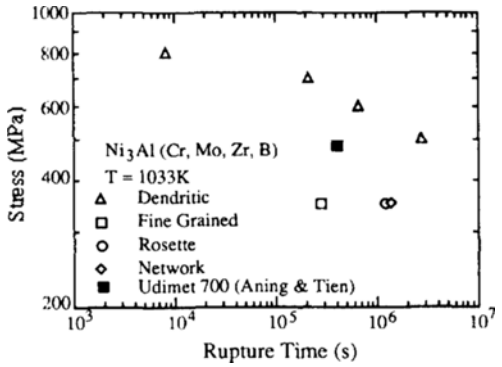

Fig. 8 Creep rupture lifetimes for different microstructures as a function of applied stress

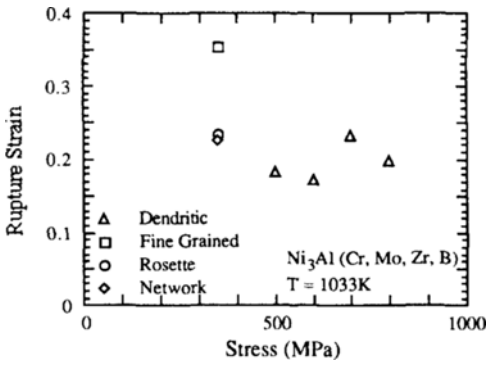

Fig. 9 Rupture strain for specimens with different microstructures as a function of applied stress

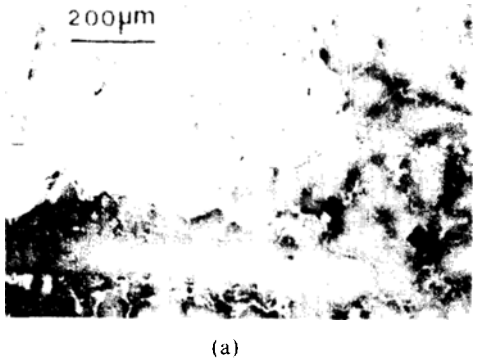

(a)

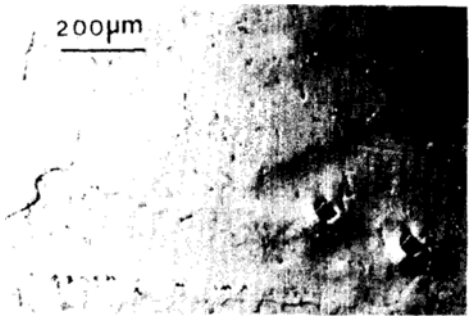

(b)

Fig. 10 The micrograph showing (a) an etched and (b) unetched cross-section of the dendritic microstructure for a specimen tested under 600 MPa at 1033 K. The tensile stress axis is in the vertical direction for this micrograph

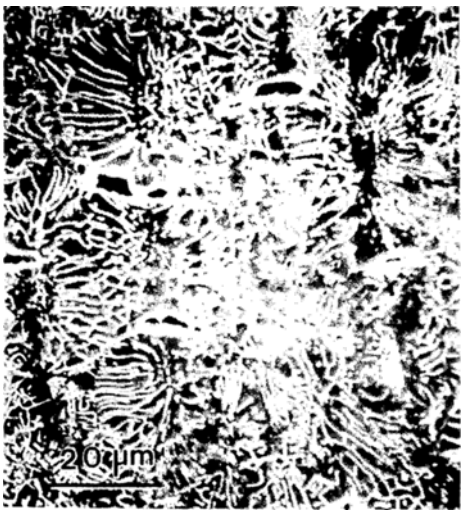

Fig. 11 The micrograph showing a polished cross-section of the rosette microstructure of interrupted specimen tested under 350 MPa at 1033 K. The tensile stress axis is in the vertical direction for this micrograph

specimen tested under 600 MPa to a strain of 0.08. Comparison of these micrographs indicates that cavity nucleation and growth, shown in the unetched micrograph, primarily occur at interdendrite boundaries, shown in the etched micrograph. Thus, it appears that creep rupture in the dendritic material is facilitated by the formation of interdendrite cavities, leading to microcrack along the interdendritic boundaries. In the cases of the rosette and network microstructures it has been shown that a large number of cavities exist on the grain boundaries that are denuded of γ phase and nearly transverse to the applied stress axis. Figure 11 shows an example of creep cavity damage in a specimen with the rosette microstructure which was tested under 350 MPa.

Some insight into the reason for the marked differences in creep fracture behavior may be obtained from SEM micrographs of the rupture surfaces. The fracture surface for the dendritic material, as shown in Fig. 12, typically exhibits both intergranular and transgranular fracture modes. This is evidenced by the observation that size and shape of the small islands on the fracture surface are the same as the size and shape of solidified secondary dendrite arms. In addition,

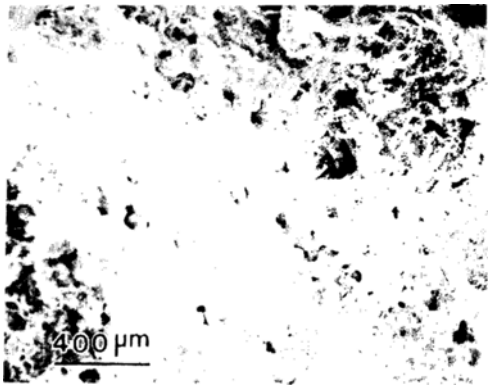

Fig. 12 SEM micrographs of the rupture surfaces for a dendritic specimen tested under 600 MPa

the spacing of these islands is equal to the secondary dendrite arm spacing. It appears that although the majority of the dendrite rupture surface area indicates transgranular failure, the formation of interdendritic microcracks by cavity coalescence initiates the creep rupture process. It is reasonable that the interdendrite boundaries in the present material are preferred sites for cavity initiation and growth just as are grain boundaries in equiaxed grain structures as a result of faster diffusion along the boundaries. It also appears that the dendrite microstructure of the alloy was reasonably stable under the present conditions, and that fracture occurred as a result of nucleation, growth and coalescence of cavities at interdendritic boundaries.

4. Discussion

As mentioned above, inverse creep is observed at small strains for Ni_3Al. Ni_3Al generally exhibits a normal primary creep response indicating material hardening followed by an accelerating or inverse creep rate which has a minimum at relatively small strain and then followed by steady state behavior (Stoloff, 1989). In general, this inverse creep phenomenon can be attributed to relatively low initial dislocation density. Kear showed that the inverse creep was completely eliminated presumably due to the instantaneous generation of a (112) dislocations in the presence of the shock-induced substructure (MacKay et al.,

1985). This supports the idea that the inverse creep is caused by a combination of the low initial dislocation density and absence of easily activated dislocation sources. When dislocations are initially present throughout the sample, the inverse creep disappears and is replaced by the usual primary creep stage with a high initial creep rate which eventually decreases to turn into a constant rate corresponding to the secondary stage. Recently, Hemker(1991) suggests that the inverse creep of Ni_3Al is caused by the glide of dislocations on the (010) cube cross-slip plane. The intermediate temperature of creep deformation is initiated by the glide of super-partial dislocation pairs on the primary and secondary octahedral planes, (111) and ($\bar{1}$11). The thermally activated cross-slip of screw segments onto the (010) plane in the form of Kear-Wilsdorflocks(Hemker, 1991) render these dislocations immobile and this leads to the exhaustion of octahedral glide. However, the KW locks formed during primary creep serve as sources for dislocation generation and motion on the (010) cube cross-slipped dislocations are able to bow out and glide on the (010) plane. The production and multiplication of dislocations on the (010) plane leads to an ever increasing creep rate and inverse creep. However, as mentioned before, this material is not fully ordered ; both Ni_3Al (γ') and Ni-rich (γ) phases exist. It could be speculated that the disordered γ phase of low melting interdendrite phase might result in a change in dislocation slip features or that there were high initial dislocations on the cube slip planes to effectively bypass this process during creep.

The steady state creep rates in many materials can be described by a power law creep expression.

$$\dot{\varepsilon}_s = A\sigma^n \exp(-Q/RT) \tag{2}$$

where A is a material constant and RT has the usual meaning. In many pure metals and solid solution alloys, the stress exponent n is usually between 3 and 5 and the activation energy for creep Q is close to the value for self diffusion (Mukherjee et al., 1985). Particle strengthened systems, however, are often characterized by unusually high values for these two parameters. In γ' strengthened nickel-based superalloys, values of n in the range of 7 to 15 and apparent activation energies up to three times that for self diffusion have been reported (MacKay et al., 1985). For the present Ni_3Al alloy with the dendritic microstructure, the value of stress exponent increases from 6 to 20 with stress. The change in stress exponent can be attributed to a change in the deformation mechanism. The value of stress exponent, $n(=6)$, at intermediate stress ranges, is lower than those generally determined for Ni-base superalloys. It is often found that by increasing the matrix strength through solute element additions instead increasing the particle resisting stress, stress exponent will be lowered. In the case of the dendritic material the strengthening mechanism is likely by solid solution strengthening instead particle or precipitate strengthening. That might be lower stress exponent than that for typical superalloys at intermediate stress regions. Generally, for superalloys at the intermediate stress ranges the dislocations created are unable to cut through the γ' particles, and climb occurs until loop reaches critical width, because the stress values are less than those required for cutting or bowing around γ' particles. At the high stress ranges the dislocations generated at a source may cut or bow between γ' phase. When the applied stress is too low for significant dislocation glide to have occurred, the alloy creeps by diffusional processes.

In attempting to identify the primary cause of the accelerating strain rate during tertiary creep it is helpful to consider the damage tolerance parameter, λ, defined as

$$\lambda = \frac{\varepsilon_f}{\dot{\varepsilon}_{\min} t_r} \tag{3}$$

where ε_f is the rupture strain, $\dot{\varepsilon}_{\min}$ is the minimum strain rate and t_r is the time to rupture. Dyson and Leckie(1988) have proposed that alloys which fail by diffusive cavitation exhbit very little strain softening and generally have λ values that lie between 1 and 2.5. They also suggest that microstructural softening results in larger values of λ. For all the present materials, as shown in Fig. 13, λ is in the range of 1~3,

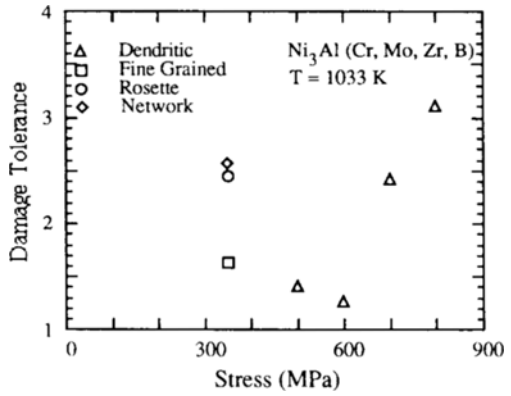

Fig. 13 Creep damage tolerance for different microstructures as a function of applied stress

indicating that strain softening is negligible and that tertiary creep is primarily a result of cavitation damage, and that the intergranular cavitation and cracking are mainly responsible for the creep rupture. Also, it is interesting to note that due to the stability of the microstructures the values of λ for the present material with different morphologies are much lower than are typically measured for nickel-base superalloys which microstructurally soften during creep (MacKay et al., 1985).

We have observed that grain morphologies in Ni_3Al alloys produced by thermal/mechanical treatment can have substantial effect on high temperature performance. In particular, the best combination of properties are exhibited by a dendritic microstructure. One explanation for this finding could be that a crystallographic texture exists in the dendritic material which is unfavorable for dislocation creep for the loading conditions imposed. However, an observed variation in the orientation of the secondary dendrite arms with respect to the stress axis suggests that the present dendritic structure is not strongly textured. Further work will be performed using X-ray diffraction techniques to examine whether texture exists in the dendritic microstructure.

Another possible explanation for the superior properties of the dendritic microstructure can be found by considering the effect of grain boundary sliding in the equiaxed grain structures. In addition to contributing to the overall strain, grain boundary sliding can lead to a substantial redistribution of stresses from sliding boundaries where sliding does not take place (Hsia et al. 1991). As a result, sliding may have two detrimental effects : 1) accelerated creep deformation within the grain interiors and 2) accelerated cavity growth and coalescence on transverse boundaries. These effects are consistent with the experimental data and microstructual observations in the present investigation considering the inability for sliding to take place in the dendritic structure. Also, the propagation of microcracks formed by cavity coalescence is probably impeded by the neighboring secondary dendrite arm because of difficulty associated in propagating the crack along such a boundary. Comparison of specimen cross-sections for all of the microstructures produced in the present investigation showed that for a given stress there was a smaller proportion of cavitated grain boundaries in the dendritic material.

On the basis of characterizations by metallography it is suggested that the extended lifetimes of the Ni_3Al specimens might be partially due to the fact that little or no boundary sliding would occur in the dendritic microstructure. Thus, the stresses within the microstructure would remain more uniform.

5. Conclusions

Based on the results of high temperature creep deformation and fracture in a Ni_3Al alloy of different microstructures produced by thermomechanical treatments at 1033 K under vacuum, the following conclusions are made,

(1) The creep strength of a dendritic microstructure in Ni_3Al (Cr, Mo, Zr, B) is considerably greater than that for other microstructures having an equiaxed grain morphology.

(2) In the case of dendritic material the stress exponent for power law creep changes from 6 to 20 with stress. The change in stress exponent can be attributed to a change in the deformation mechanism.

(3) Specimens with the dendritic microstructure exhibited substantially longer creep lifetimes than those for the specimens with equiaxed grains.

From the microstructural observations, it is concluded that the segments of dendritic boundaries that are roughly normal to the applied stress are the preferred cavity nucleation sites. This results in isolated interdendritic cavitation in the absence of grain boundary sliding which, in turn, leads to rupture lifetime that are longer than those observed for the other microstructures.

References

Aning, K. and Tien, J. K., 1980, "Creep and Stress Rupture Behavior of a Wrought Superalloy in Air and Vacuum," *Journal of Materials Science and Engineering*, Vol. 43, pp. 23~33.

Bendersky, L., Rosen, A. and Mukherjee, A. K., 1985, "Creep and Dislocation Substructure," *International Materials Reviews*, Vol. 30, pp. 1~15.

Dyson, B. F. and Leckie, F. A., 1988, "Physically Based Modeling of Remaneent Creep Life," *Materials Science and Engineering*, A 103, pp. 111~114.

Hemker, K. J., 1991, "A Study of High Temperature Deformation in the Intermetallic Alloy Ni_3Al," Ph. D Dissertation, Stanford University.

Hsis, K. J., Parks, D. M. and Argon, A. S., 1991, "Effect of Grain Boundary Sliding on Creep Constrained Boundary Cavitation and Creep Deformation," *Mechanics of Materials*, Vol. 11, pp. 43~62.

Izumi, O. and Takasugi, T., 1988, "Mechanisms of Ductility Improvement in Ll 2 Compounds," *Journal of Materials Researches*, Vol. 3, pp. 426~440.

Lall, C., Chin, S. and Pope, D. P., 1979, "The Orientation and Temperature Dependence of the Yield Stress of Ni_3(Al, Nb) Single Crystals," *Metal Transaction*, Vol. 10A, pp. 1323~1332.

Liu, C. T., White, C. L. and Horton, J. A., 1985, "Effect of Boron on Grain Boundaries in Ni_3 Al," *Acta Metallurgica*, Vol. 33 pp 213~229.

Milligan, W. W. and Antolovich, S. D., 1989, "On the Mechanism of Cross Slip in Ni_3Al," *Metall Transaction*, Vol. 20A, pp. 2811~2818.

Schneibel, J. H. and Martinez, L., 1989, "Crack-Like Creep Cavitation in a Nickel Aluminide," *Acta Metallurgica*, Vol. 37, pp. 2237~2244.

Stoloff, N. S., 1989, "Physical and Mechanical Metallurgy of Ni_3Al and Its Alloys," *International Materials Reviews*, Vol. 34, pp. 152~183.

Yamaguchi, Y and Umakoshi, 1990, "The Deformation Behavior of Intermetallic Superlattics Compounds," *Progress in Materials Science*, Vol. 34, pp. 1~148.